

Construction and Operation of an Internal Coil Device, RT-1, with a High-Temperature Superconductor

Yuichi OGAWA, Zensho YOSHIDA, Junji MORIKAWA, Haruhiko SAITO, Sho WATANABE, Yoshihisa YANO, Shoichi MIZUMAKI¹⁾ and Taizo TOSAKA¹⁾

Graduate School of Frontier Sciences, The University of Tokyo, Kashiwa, Chiba 277-8568, Japan

¹⁾*TOSHIBA corporation, Yokohama 230-0045, Japan*

(Received 30 December 2008 / Accepted 9 March 2009)

An internal coil device called Ring Trap-1 (RT-1) has been constructed to explore an innovative concept for a high-beta plasma based on a new relaxation theory. A high-temperature superconductor (HTS) Bi-2223 tape is employed for the internal coil of RT-1. The coil is cooled to 20 K with helium gas supplied by G-M refrigerators, and charged to a magnetomotive force of 250 kA using an external power supply. For these cooling and charging methods, we have developed several innovative techniques such as a demountable transfer tube system, persistent current switch, detachable electrode, and others. In addition, we have paid much attention to the deterioration of the HTS tape during the fabrication of the internal coil. As a result, we have demonstrated that the decay of the persistent current of the internal coil is $\sim 1\%$ during 8 h. The internal coil is lifted with a levitation coil located at the upper region of the vacuum vessel. The coil position monitored with laser sensors is feedback controlled through the regulation of the levitation coil current. Stable levitation for a few hours has been demonstrated for various plasma experiments.

© 2009 The Japan Society of Plasma Science and Nuclear Fusion Research

Keywords: internal coil device, high temperature superconductor, persistent current switch, magnetic levitation, relaxation theory, high-beta plasma

DOI: 10.1585/pfr.4.020

1. Introduction

Plasma flow (i.e., ion flow) is one of the key parameters in understanding plasma dynamics. J.B. Taylor developed a relaxation theory based on plasma current (i.e., electron flow) to explain RFP plasmas. If plasma flow is introduced into the relaxation theory, a new self-organized state is expected. S.M. Mahajan and Z. Yoshida have developed a two-fluid relaxation theory by taking the effect of plasma flow into account, and a new relaxation state has been identified [1, 2]. This self-organized state has the potential to confine a high-beta plasma by utilizing a strong plasma flow. Self-organization related to a relaxation phenomenon is observed in many other scientific fields, and is one of the most crucial issues in contemporary science. The observations of several spacecrafts have shown that a high-beta plasma is confined on Jupiter with a dipole magnetic configuration [3]. A. Hasegawa has proposed a theory to explain this high-beta plasma [4], where relaxation in the phase space is taken into account by the conservation of several adiabatic constants. Based on this theory, he has proposed a fusion reactor with a dipole magnetic field [5].

Recently, internal coil devices have been coming to the forefront for exploring a new frontier in plasma physics related to these relaxation theories. An internal coil device is suitable for studying a self-organized structure with strong plasma flow. By inducing a radial electric field,

strong plasma flow would be induced in the toroidal direction by $V_t = E_r/B_p$. We therefore expect to confine high-beta plasmas by utilizing this plasma flow.

Inspired by these new relaxation theories, internal coil devices were constructed in the 1990s, e.g., the Ring Trap (RT)-series devices at the University of Tokyo [6] and the Levitating Dipole eXperimental (LDX) device [7] as a joint project between Massachusetts Institute of Technology and Columbia University.

In the 1970s, there were several internal coil devices, such as a spherator, a levitron, and an octapole, and plasma experiments with a levitated superconductor coil were carried out [8]. The main purposes of the 1970s-era research were focused on neoclassical transport, MHD physics such as an averaged minimum- B , magnetic shear, and so on. Therefore, the plasma was mainly produced and confined at the inner region of the torus. On the other hand, in the 1990s, the internal coil devices were constructed at the University of Tokyo and MIT/Columbia University to study high-beta plasma based on the new relaxation theories. These projects have a quite different purpose from those using the previous internal coil devices, and the plasma itself is confined at the outer region of the torus. Figure 1 compares an internal coil device of the 1970s and a recent device, noting the plasma confinement region and the controllability of the floating coil.

At the same time, progress in high-temperature super-

author's e-mail: ogawa@ppl.k.u-tokyo.ac.jp

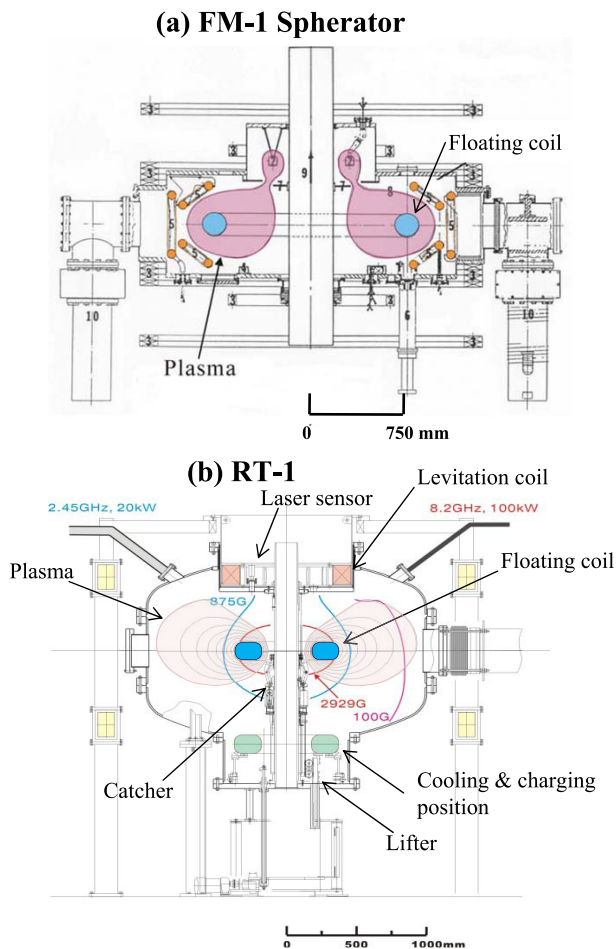


Fig. 1 Comparison between the FM-1 spherator and RT-1. The confinement region is different between the two devices, i.e., the inner region of the torus in the FM-1 spherator and the outer region in RT-1.

conductors (HTS), especially BSCCO tapes, is quite remarkable [9]. As long BSCCO tapes of more than a few hundred meters are available, large coils have been constructed in a device for silicon crystal growth [10] and a MAGLEV project [11]. In fusion reactors, the feasibility of applying an HTS coil has been studied [12], since a high-field magnet with > 20 T will be available if the HTS coil is used.

Several internal coil devices have been constructed at the University of Tokyo. Z. Yoshida has initiated plasma experiments with the internal coil device Proto-RT, which has a normal conductor with a coil major radius of 300 mm and a magnetomotive force of 10 kA [13]. Next, an internal coil device called Mini-RT has been constructed, which is the first fusion plasma experimental device equipped with an HTS. The magnetomotive force of this HTS coil is 50 kA [14]. Now a new device, RT-1, with a relatively large HTS coil has been constructed.

In this paper, the construction and operation of RT-1 are summarized. In Sec. 2, the characteristics of RT-1

are presented, paying much attention to advantages and research and development issues for employing an HTS coil in an internal coil device. The specifications and performance of several key components are described in Sec. 3. Operational results of RT-1 are presented in Sec. 4. A brief summary is given in Sec. 5.

2. Characteristics of RT-1

2.1 Application of HTS for the internal coil

In internal coil devices constructed around 1970, e.g., the spherator, levitron, and octapole, a low-temperature superconductor (LTS) such as NbTi or Nb₃Sn was used in a floating coil. HTS materials were discovered in 1986, and many applications have been explored. If an HTS tape is available for the internal coil, there might be several advantages:

- The HTS coil needs to be cooled to only about 20 K for achieving satisfactory performance. This results in the possibility of a helium gas cooling system with a G-M refrigerator. A cooling system without liquid helium might be quite convenient for operation of the device itself.
- The operational temperature range can be remarkably expanded because the critical temperature of HTS is quite high (typically ~ 100 K or more). For example, in RT-1, the HTS coil is initially cooled to ~ 20 K, and a temperature of up to ~ 40 K is feasible for coil operation; i.e., a temperature increase of ~ 20 K is acceptable. This characteristic is quite important for the internal coil device because there is no active cooling of the coil during plasma experiments.
- The specific heat capacity near ~ 20 K is much larger than that near ~ 4 K. This is another advantage of the HTS coil compared with the LTS one. In the LTS coil case, helium gas at a pressure of more than 100 atmospheres at room temperature is usually fulfilled inside the internal coil as a heat reservoir. In the HTS coil case, it might be unnecessary to introduce a special heat reservoir because the coil has a large heat capacity at ~ 20 K. This advantage of the HTS coil might make it possible to prolong the plasma experiment period, in addition to enabling a remarkable relaxation of the thermal shield design of the internal coil.

However, we should pay attention to the following problems of using an HTS coil:

- Current density in an HTS is lower than that in an LTS. This might result in an increase in the cross section of the wound HTS tape in the internal coil.
- The electric resistance due to the flux flow loss is not small. This might limit the duration of the persistent current in the HTS coil.
- The winding technology for HTS coils is not yet established and the cost of the HTS tape is high, compared with those of LTS coils.

From these considerations, we have decided to employ the HTS tape for the internal coil in RT-1. BSCCO and YBCO might be candidates for the HTS material. We have a quite long BSCCO tape with a length of a few hundred meters, and the coil winding technology has been developed in several cases such as a device for silicon crystal growth [10], MAGLEV [11], and Mini-RT [14]. In contrast, the fabrication capability and winding technology for YBCO are not yet well developed. Therefore, we have employed BSCCO for the HTS coil in RT-1.

2.2 Excitation method of the internal coil

The induction method has been employed for coil excitation in past internal coil devices, including the LDX device, because the coil should be excited inside the vacuum vessel. However, it is necessary to furnish an induction coil that is capable of producing a magnetomotive force of 2-3 times that of the internal coil.

The switchover between the superconducting and normal conditions of an LTS is easily controllable by introducing a small change in the coil temperature. However, the temperature of an HTS coil has to be elevated to the level of normal conditions (typically, more than 100 K) during the excitation of the induction coil, and the coil should be re-cooled to the operational temperature (~ 20 K for RT-1). It takes a few hours for this re-cooling of the HTS coil.

To overcome these problems, we have decided to use a persistent current switch (PCS) inside the internal coil. Since an induction coil is not required, a remarkable reduction in the required power can be expected. In addition, large variations in the HTS coil temperature during coil current excitation can be avoided, and the excitation period could be remarkably shortened.

In the Mini-RT device, a PCS made of a Bi-2223 tape has been developed [15]. The switchover time is governed by the cooling time of the PCS from the switch-off temperature (typically > 100 K) to the switch-on temperature (< 30 K). Since the PCS in the Mini-RT is made of a small coil with a few turns of the Bi-2223 tape, it takes ~ 10 min for the switchover. In contrast, in the MAGLEV project, a PCS made of a YBCO thin film has been developed [16]. Since this PCS is a thin film, the switchover time is quite short, typically 2 min. In RT-1, therefore, we have employed a YBCO thin film for the PCS.

2.3 Cooling method

At first, we considered direct access to the HTS itself through the thermal shield region from the outer surface of the internal coil, because direct cooling of the HTS through the cold head of the refrigerator is quite effective and reliable if it is available. On the other hand, since the internal coil is isolated from the cryogenic cooling system during plasma experiments, the HTS itself should be carefully shielded from thermal load from the outer surface of the internal coil. However, it is quite difficult to have both

high performance of the thermal shield during the operation period and a good heat conduction path to the HTS during the cooling period.

Here we have decided to employ a cooling system with cooled helium gas directly guided inside the internal coil. The helium gas is cooled using G-M refrigerators. For this purpose, we have developed a demountable transfer tube system.

2.4 Floating system

A floating coil is unstable for several motions such as up-down, tilting, and sliding movements. The magnetic lift-up technique is adopted for levitation of the internal coil. Since the floating coil is unstable only in the vertical direction in the lift-up method, the external control of only one parameter (i.e., vertical motion) is sufficient for stable operation of the internal coil. The coil position is measured with laser position sensors placed at the top of the torus, and the levitation coil current is feedback controlled to maintain the coil position for a few hours.

In an accidental failure, the internal coil should be safely recovered by some mechanical support system. Here we have equipped a catcher system with several arms, which is attached at the center column of RT-1. All arms are normally flattened against the center column. When the position control of the floating coil fails, all arms unfold quickly to catch the falling coil.

2.5 Overview of RT-1 and operation scenario

Characteristics and machine parameters of RT-1 are summarized in Table 1. Figure 1(b) shows a cross-sectional view of RT-1, and Fig. 2 is an overview of RT-1, including the main components.

Initially the internal coil is positioned at the bottom of the vacuum vessel so as to cool down and excite the HTS coil. The transfer tubes, electrode, and multi-pin connectors are inserted into the internal coil from the bottom of the vacuum vessel. For these attachment processes, the coil position is precisely adjusted with a rotating stage.

When coil current excitation is complete, the internal coil is pushed up to the middle position of the vacuum vessel with a mechanical lifter. The levitation coil located outside of the vacuum vessel is excited to allow the internal coil to be levitated, and coil position is monitored with laser position sensors located at the top of the torus.

Table 1 Specifications of RT-1 in comparison with LDX.

	RT-1	LDX
Floating coil	HTS tape (Bi-2223)	LTS (Nb ₃ Sn)
Levitation method	Lift-up	Lift-up
Excitation	Direct charging	Induction
Cooling	20 K helium gas	4 K liquid helium

During plasma experiments, the lifter is pulled down at the bottom of the vacuum vessel. Just after the end of plasma experiments, the internal coil is recovered by the lifter.

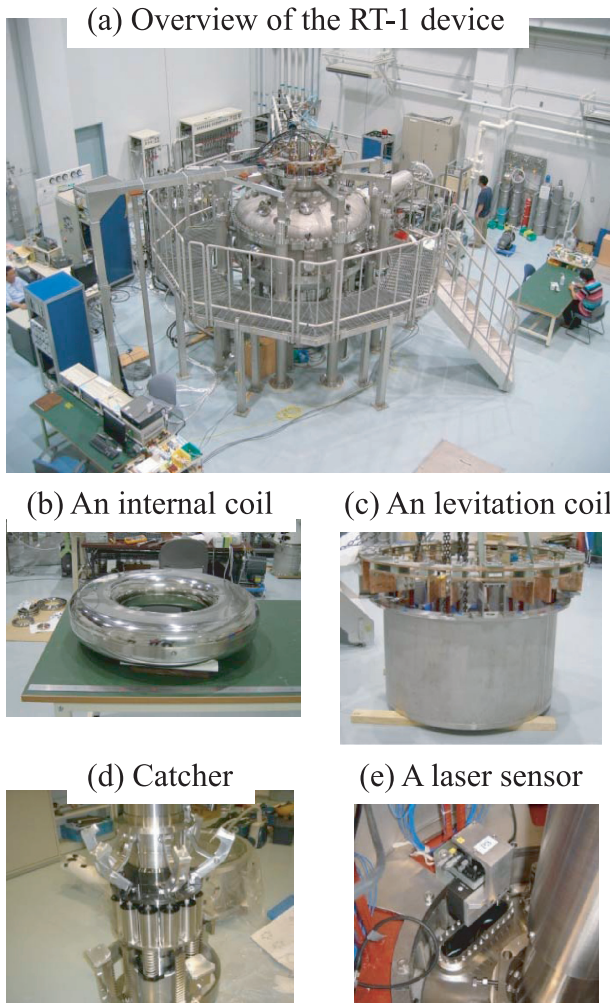


Fig. 2 Overview of (a) RT-1 and several key components: (b) an internal coil, (c) a levitation coil, (d) catcher, and (e) a laser sensor.

The operation scenario is schematically drawn in Fig. 3 with the corresponding coil temperatures. At first, it might take ~ 2 days to cool down the HTS coil from room temperature. Here we have monitored the coil temperature at several positions, and the cooling rate is controlled to keep the temperature difference to less than 20 K at various coil positions to avoid a large thermal stress. After an initial cooling of the coil, a pair of retractable current leads is connected to the internal coil, and a YBCO thin film is heated to open the PCS. The internal coil is excited up to the nominal current with an external power supply for ~ 10 min. Then the heater current is turned off, and the YBCO thin film is re-cooled, resulting in the switch-on condition of the PCS. By reducing the external coil current to zero, a persistent current mode is established in the circuit of the HTS coil and the PCS. Since the HTS coil temperature increases slightly (typically $\Delta T \approx 5$ K) during this excitation process, the HTS coil is re-cooled as shown in Fig. 3. It takes 1 h for this re-cooling.

Just before the internal coil is lifted, the helium gas inside the transfer tube is evacuated, and a pair of detachable transfer tubes is disconnected from the internal coil. During plasma experiments, which are expected to last 8 h, the HTS coil temperature increases gradually. The thermal shield of the internal coil is designed to limit the temperature increase to 10 K (e.g., from 20 to ~ 30 K).

Just after plasma experiments, the internal coil goes back to the bottom of the vacuum vessel, and the coil current is discharged to the external power supply. In this period, the transfer tube is not connected to the coil. Since the transfer tube is warmed to room temperature during a few hours of plasma experiments, the helium gas would be warmed by the heat load through the transfer tube. After discharge of the coil current, the transfer tube is connected to the internal coil, and cooling to 20 K is carried out for the next plasma experiments. This experimental cycle, i.e., from the excitation of the HTS coil to discharge and re-cooling after plasma experiments, is repeated day by day.

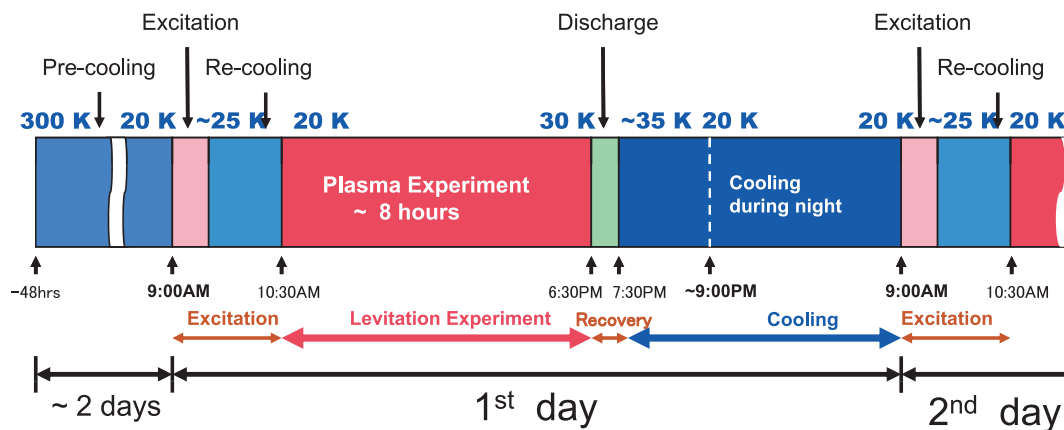


Fig. 3 Schematic behavior of the coil temperature based on the routine operational scenario.

3. Design Specification and Performance of Each Component

3.1 High-temperature superconductor tape

The specifications of the internal coil are listed in Table 2, and a schematic drawing is shown in Fig. 4. Here we employed an Ag-sheathed Bi-2223 tape manufactured by pressurized sintering. Table 3 shows the characteristics of the Bi-2223 tape, where the critical current is in the range of 100-120 A at 77 K, s.f., 1 μ V/cm, and the length of each tape is \sim 400 m. Since the residual resistance is quite important for the persistent current mode, we have paid much attention to the n -value of the Bi-2223 tape, where n -value

Table 2 Specifications of the floating HTS coil.

HTS tape	Ag-sheathed Bi-2223 tape
Coil radius	$R_c = 0.25$ m
Winding method	Single pancake
Stack number	12 pancakes
Magnetomotive force	$I_{m.f.} = 250$ kA
Coil current	$I_c = 115.6$ A
Coil inductance	$L_c = 3.3$ H
Stored energy	$W_{energy} = 22$ kJ
Coil weight	110 kg
Operation temperature	20-40 K
Maximum magnetic field	$B_{\perp} = 1.12$ T $B_{//} = 1.57$ T

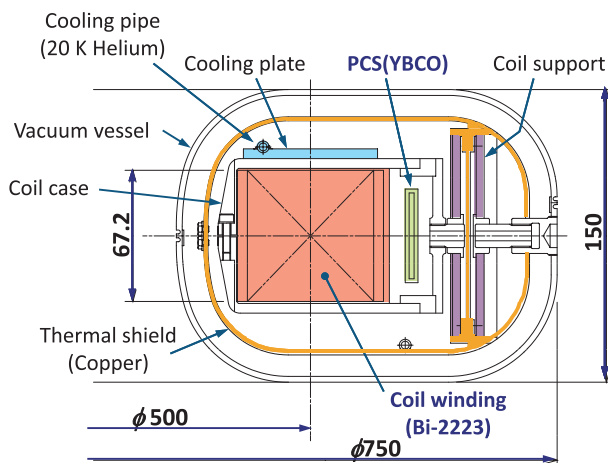


Fig. 4 Cross section of the floating coil.

Table 3 Characteristics of the HTS conductor.

Tape size	thickness, 0.23 ± 0.03 mm; width, 4.2-4.6 mm
Critical current	> 100 A at 77 K, s.f. 10^{-6} V/cm
n -index	> 18 (10^{-9} - 10^{-6} V/cm)
Silver ratio	1.5
Tensile strength	> 100 MPa

is defined by $V = V_c(I/I_c)^n$, and the residual resistance has been measured up to a range of 10^{-9} V/cm. In addition, deterioration of the n -value in the winding process is a concern. The n -value has been measured for all twelve single pancake coils, and it was confirmed that the residual resistances were less than 10^{-9} V/cm for each coil.

A double pancake is produced by connecting two single pancakes with a silver plate at the inner side of the coil. Six pairs of double pancake coils are stacked in RT-1 and connected at the outer side of the coil. We paid attention to minimize the magnetic field produced by these connection lines, because an error field would induce deterioration of the magnetic field for the plasma confinement and rotation of the floating coil in the toroidal direction. As a result, by properly distributing the connection lines in the toroidal direction, the maximum magnetic field error on the surface of the internal coil is suppressed to less than 0.2% of the dominant dipole field [17].

As shown in Fig. 4, the HTS coil is covered with a thermal shield made of copper, and the HTS coil and thermal shield are wrapped in super-insulation. The HTS coil is directly supported through the vacuum vessel of the internal coil, by paying attention to not only enhance mechanical strength but also reduce the thermal load [18].

The maximum magnetic field perpendicular (parallel) to the Bi-2223 tape is 1.12 T (1.57 T). This results in deterioration of the critical current of the HTS tape, while operation at a reduced temperature (e.g., \sim 30 K at most) might increase the critical current. By taking these two effects into account, the critical current of the HTS coil in RT-1 is estimated to be 223 A. Because the operation current is set to 115.6 A, the load rate of the HTS coil is 52%.

3.2 Cooling system

Three G-M cryocoolers with \sim 50 W in total at 20 K are prepared, and a helium circulation compressor supplies cooled helium gas with a mass flow rate of 2 g/s to the HTS coil through the transfer tube. The helium gas is pressurized to 5 atmospheres.

A demountable transfer tube system is developed. In the Mini-RT device, an organic seal of Kel-F was employed, and careful connection of the check valve was required. In RT-1, a VCR connection with a metal gasket is employed. The VCR connection is operated from outside of the vacuum vessel with a double Wilson sealed structure [18].

3.3 Excitation scenario and PCS

As shown in Fig. 4, a PCS made of a YBCO thin film on a sapphire substrate is attached on the outer surface of the HTS coil; the characteristics of this PCS are listed in Table 4. By elevating the temperature of this YBCO thin film to 100 K, an electric resistance of 0.67Ω is generated, resulting in the switch-off condition. This YBCO thin film is cooled by thermal conduction through the HTS coil, be-

Table 4 Characteristics of the HTS PCS.

Conductor	YBCO thin film
Size	thickness, 300 nm; width, 6 mm; line length, 76 mm
Critical current	$I_c = 254$ A at 30 K, 1 T
Off resistance	0.67 Ω
Operation time	On to off : 29 s Off to on : 126 s

cause the film is thermally connected to the cooling plate with an aluminum strip. The cooling period from 100 K to less than 30 K is 1-2 min.

The stored energy of the HTS coil should be damped by the resistance in the case of the HTS coil quench. A damping resistance of 60 m Ω is prepared inside the coil vacuum vessel and connected to the HTS coil in parallel with the PCS [19].

A detachable current lead has been developed. A MultilamTM contact is employed for the current lead joint. The socket contact inside the internal coil is configured using two components, which are independently supported by the coil vacuum vessel and the coil casing. These two components are electrically connected by inserting the head of the current lead joint. Since the current lead is thermally connected to the HTS coil, heat leakage from the electrode to the HTS coil would increase considerably. To reduce the heat load to the HTS coil, the current lead is cooled by helium gas with a temperature of ~ 80 K, which is supplied from the first stage of the G-M refrigerator.

Contact resistance is a concern for this current lead joint. We have repeated a test of the contact resistance ~ 1000 times and confirmed that the contact resistance is about 200 $\mu\Omega$. This yields a heat load of 2.7 W, which is acceptable [18].

3.4 Position control of the floating coil and safety system in failure mode

The specifications of the levitation coil are listed in Table 5. The coil's maximum current is approximately 1300 A, and the feedback control can apply ± 150 A with a dynamic range of < 20 Hz (a switching regulator is used to control the current). Research and development of magnetic levitation systems have previously been carried out on the FB-RT and Mini-RT devices [19]. Since the HTS coil of RT-1 is suspended by a levitation coil located above the chamber, the floating coil is unstable in its vertical motion. Feedback control of the levitation coil current is applied for dynamic stabilization of the floating coil. The vertical position of the floating coil is measured with laser sensors, and the position signal is processed with an analog proportional-integral-derivative controller.

The floating coil has six degrees of freedom. Since rotation in the toroidal direction does not affect the dipole

Table 5 Specifications of the levitation coil.

Conductor	copper
Radius	$R_L = 0.4$ m
Coil position	$Z = 0.612$ m from the floating coil
Coil size	width, 0.126 m; height, 0.157 m
Total turn number	68
Resistance	$R_{\Omega,L} = 26$ m Ω
Inductance	$L_L = 4.6$ mH
Coil current	$I_L = 1300$ A
Magnetomotive force	$I_{m.f.} = 88.4$ kA

magnetic field, we should control the other five degrees of freedom, i.e., (x , y , z) motions and x -axis and y -axis rotations. To measure these five motions, five-code laser sensors are required. At present, however, three sensors mounted on the top of the vacuum vessel are sufficient to control the floating coil, because the sliding motions in the x and y directions are stable in the lift-up method. Each sensor has an accuracy of 50 μm and a response time of 1 ms. The vertical position and the tilt angles (θ_x , θ_y) in the x and y axes are detected by these three detectors [20].

In the emergency case of a loss of control, a catcher system operates to hold the coil within 100 ms (during which the coil falls freely about 50 mm in distance). This catcher system consists of several arms. Each arm is connected to the cylinder, and the shock is absorbed by the friction force of this cylinder to avoid damage to the coil. This catcher system, mounted on the center column of RT-1, is shown in Fig. 2, where the coil is caught on the unfolded arms.

4. Operation of RT-1

4.1 Cooling and excitation of the HTS coil

The cooling pipe is mounted on the upper surface of the HTS coil, and helium gas cooled by the G-M refrigerators is guided into this pipe. The HTS coil temperature is measured at several positions inside the internal coil. The gas flow rate is regulated to keep the maximum temperature difference to less than 20 K using the heater installed at the refrigerator line. Usually it takes ~ 2 days to cool the HTS coil from room temperature to the 20 K range.

First, we examined the performance of the thermal shield of the internal coil. Just after cooling down to ~ 20 K, the transfer tubes were disconnected from the internal coil, and the spontaneous temperature increase in each component inside the internal coil was monitored. After 8 h, the temperature of the HTS coil increased to ~ 30 K and that of the thermal shield to ~ 100 K. This confirms that the performance of the thermal shield might be satisfactory for plasma experiments [17].

An experimental result of the HTS coil excitation is shown in Fig. 5. First, the PCS heater is switched on for

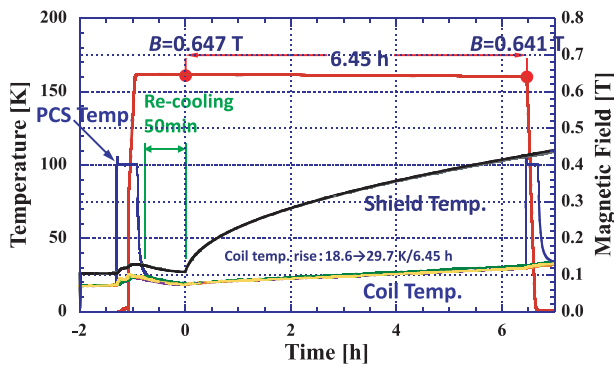


Fig. 5 Experimental results for HTS coil excitation. The excited coil is kept for 6.45 h at the persistent current mode with no supply of cooled helium gas.

excitation of the HTS coil, and it takes about 1 min to reach 100 K. The temperature of the PCS is regulated to be 100 K to maintain the switch-off condition. The HTS coil current is excited by the external power supply at a rate of 0.2 A/s. Since the rated current of the HTS coil is 115.6 A, it takes ~ 10 min for the excitation of the HTS coil current. Next, the PCS heater is immediately switched off, and the PCS is gradually cooled through conduction cooling from the HTS coil itself. Usually it takes a few minutes to reach a temperature of less than 25 K. After it is confirmed that the switch-on condition is established for the PCS, the current of the external power supply is decreased to zero, resulting in a persistent current mode in the circuit of the HTS coil and PCS. During this excitation process, the HTS coil temperature increases slightly because of heat input to the PCS and heat conduction from the current leads; typically the increment in the HTS coil temperature is ~ 5 K. To recover from this temperature increase, the HTS coil is re-cooled for 1 h. Just after the end of this re-cooling process, the supply of cooled helium gas is terminated. The gate valves between the refrigerators and the transfer tube are closed, and the helium gas inside the transfer tube is evacuated with a differential pumping system. The transfer tube is extracted from the internal coil, and a persistent current mode with no active cooling is established. In Fig. 5, this persistent current mode is maintained for 6.45 h, and a quite small decrease in the persistent current is observed. Since the magnetic field strength at the coil center decreased from 0.647 to 0.641 T after 6.45 h, the current decay time is estimated to be $9.3 \times 10^{-2} \%$ /h [17].

4.2 Levitation experiments and position control

After excitation of the HTS coil, the transfer tubes and multi-pin sockets are extracted from the internal coil, and the internal coil is mechanically lifted to the middle of the vacuum vessel using the lifter. With a gradual increase in the levitation coil current, the internal coil begins to launch from the lifter. The results of the levitation tests over 3 h

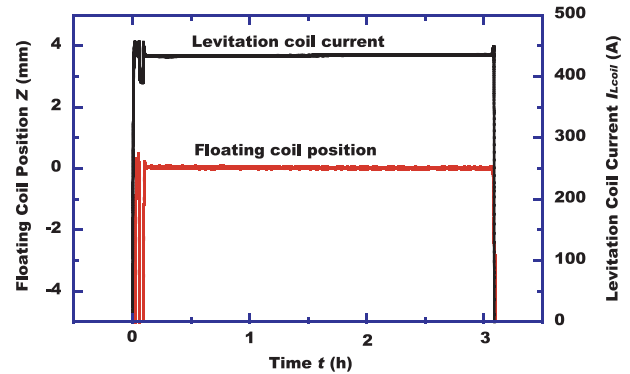


Fig. 6 Stable and long-period levitation of the HTS coil. The coil position is feedback controlled within an accuracy of $100 \mu\text{m}$ for 3 h.

are presented in Fig. 6, which shows the waveforms of the coil position measured with the laser sensor. We confirmed that the floating coil position was controlled within an accuracy of $100 \mu\text{m}$.

Incidentally, during the levitation experiments, the floating coil rotates in the toroidal direction, in addition to exhibiting a certain amount of tilt. Typically, this constant tilt angle is ~ 1 degree. The rotation and constant tilt of the floating coil might be caused by error fields due to the geomagnetic and/or the current lead of the coil and the nonuniformity of the internal coil weight in the toroidal direction.

A tilted coil creates an error field in the magnetic field for plasma confinement. To overcome these effects, two pairs of compensation coils have been mounted on the outside of the vacuum vessel. A set of opposite coils (e.g., North and South, East and West) are connected in series, and the coil currents are adjusted to compensate for the geomagnetic field.

If the weight of the coil is not uniform in the toroidal direction, a floating coil will tilt by allocating the heavier side down, and a pendulum motion will begin. A weight is put on the opposite side of the internal coil to compensate for this nonuniformity of weight. As a result, we have succeeded in controlling the floating coil position within a tilting angle of less than 0.05 degree.

Finally, if the position control of the floating coil fails, the catcher installed at the center column is expected to be open, as shown in Fig. 2. Since the falling distance of the floating coil is designed to be 50 mm, the freefall period of the floating coil to the catcher should be less than 100 ms. The time lag of the catcher system from the trigger of the failure mode signal is estimated to be 20 ms, and the mechanical operation period for opening the catcher arms is designed to be less than 80 ms. We have carried out emergency operation tests many times and confirmed the operation period of less than 100 ms with a high reliability. Once we experienced a loss of power by accident,

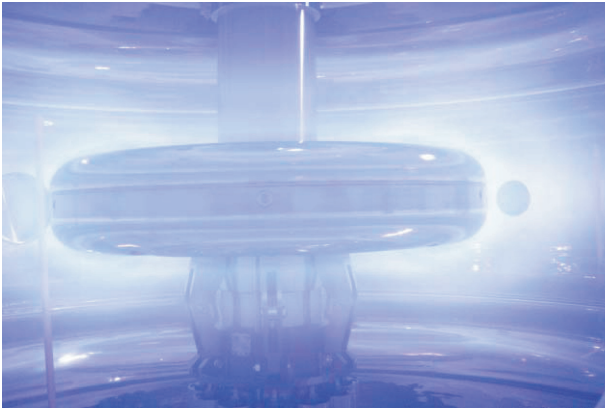


Fig. 7 [Movie] Plasma produced by 8.2 GHz microwaves, where the internal coil is floating. The pulse duration is 1 s.

and this catcher system operated smoothly, safely recovering the floating coil.

4.3 Plasma experiments

The magnetic surface in RT-1 is shown in Fig. 1 (b), where the pure dipole field is slightly modified by the levitation coil current. A separatrix appears naturally near the levitation coil, and the plasma confinement region with a separatrix is configured as shown in Fig. 1 (b). When the vertical field is introduced, the shape of the magnetic surface can be modified. In RT-1, the plasma is produced by microwaves in the electron cyclotron range of frequencies (ECRF), e.g., 8.2 and 2.45 GHz [21]. The contours of the magnetic field strength for these ECRF waves are depicted in Fig. 1 (b), as well.

Plasma produced by 8.2 GHz microwaves with a pulse length of 1 s is shown in Fig. 7. At first, we were concerned that the disturbance caused by the plasma light to the laser sensor system would affect coil position control. However, the coil position is robustly controlled for a few hours. In high-performance plasma experiments such as high-beta plasma, the floating coil position responds to the change in the floating coil current, but is smoothly controlled to the predefined position.

5. Summary

To explore an innovative concept for high-beta plasma based on a new relaxation theory, internal coil devices have been revived, i.e., RT-1 in the University of Tokyo and LDX at MIT/Columbia. In contrast to the internal coil devices of the 1970s, the plasma is confined at the outer region of the torus in these devices. We have constructed RT-1 with an HTS for the internal coil. A Bi-2223 tape (4.2–4.6 mm in width, 0.23 mm in thickness) with a critical current of more than 100 A at 77 K, s.f., $1 \mu\text{V}/\text{cm}$, is employed. The internal coil is cooled to 20 K with helium gas supplied by G-M refrigerators and charged to a magnetomotive force of 250 kA using an external power supply.

For these cooling and charging methods, we have developed several innovative techniques such as a demountable transfer tube system, persistent current switch, and detachable electrode. Since the residual resistance of the HTS tape seriously affects the decay time of the persistent current, we have paid much attention to the deterioration of the HTS tape during fabrication of the internal coil. For all pancake coils, we have imposed the requirement that the n -value of the V-I characteristics of the HTS tape should be larger than 18 in the residual resistance range of 10^{-9} – 10^{-6} V/cm. The results demonstrated that the decay of the persistent current of the internal coil is $\sim 1\%$ over the course of 8 h. The levitation coil is located at the upper region of the vacuum vessel so as to lift the internal coil. The coil position monitored with laser sensors is feedback controlled through the levitation coil current. Stable levitation for a few hours has been demonstrated for various plasma experiments.

Acknowledgments

The authors acknowledge Profs. T. Mito and N. Yanagi at National Institute for Fusion Science for designing an HTS coil and cryocooler system. The authors express their gratitude to Mr. S. Ioka, N. Tachikawa, H. Takano, M. Shibui, K. Nakamoto, T. Ono, and Y. Ohtani at Toshiba Corporation.

- [1] S.M. Mahajan and Z. Yoshida, *Phys. Rev. Lett.* **81**, 4863 (1998).
- [2] Z. Yoshida and S.M. Mahajan, *Phys. Rev. Lett.* **88**, 095001 (2002).
- [3] S.M. Krimigis *et al.*, *Science* **206**, 977 (1979).
- [4] A. Hasegawa *et al.*, *Fusion Technol.* **22**, 27 (1992).
- [5] A. Hasegawa *et al.*, *Nucl. Fusion* **30**, 2405 (1990).
- [6] Z. Yoshida *et al.*, *Trans. Fusion Sci. Technol.* **51**, 29 (2007).
- [7] LDX website, <http://psfcwww2.psfc.mit.edu/ldx/>
- [8] S. Yoshikawa, *Nucl. Fusion* **13**, 433 (1973).
- [9] K. Sato, *J. Cryo. Soc. Japan* **42**, 338 (2007).
- [10] T. Kaneko *et al.*, *IEEE Trans. Appl. Supercond.* **9**, 2465 (1999).
- [11] M. Igarashi *et al.*, *IEEE Trans. Appl. Supercond.* **15**, 1469 (2005).
- [12] P. Komarek, *Fusion Eng. Des.* **81**, 2287 (2006).
- [13] Z. Yoshida *et al.*, *Non-neutral Plasma Physics III*, AIP Conf. Proc. **498**, 397 (1999).
- [14] Y. Ogawa *et al.*, 19th Fusion Energy Conference Lyon (France), IAEA-CN-94/ICP-12 (2002).
- [15] T. Mito *et al.*, *IEEE Trans. Appl. Supercond.* **13**, 1500 (2003).
- [16] T. Tosaka *et al.*, *IEEE Trans. Appl. Supercond.* **15**, 2293 (2005).
- [17] T. Tosaka *et al.*, *IEEE Trans. Appl. Supercond.* **17**, 1402 (2007).
- [18] S. Mizumaki *et al.*, *IEEE Trans. Appl. Supercond.* **16**, 918 (2006).
- [19] T. Tosaka *et al.*, *IEEE Trans. Appl. Supercond.* **16**, 910 (2006).
- [20] J. Morikawa *et al.*, *Fusion Eng. Des.* **82**, 1437 (2007).
- [21] Z. Yoshida *et al.*, *Plasma Fusion Res.* **1**, 008 (2006).